Plant Archives Vol. 20, Supplement 1, 2020 pp. 2349-2356 **e-ISSN:2581-6063 (online), ISSN:0972-5210**

EVALUATION AND COMPARISON THE IMPLANTATION OF BOVINE URINARY BLADDER MATRIX AND POLYPROPYLENE MESH IN THE REPAIR OF CHRONIC DIAPHRAGMATIC HERNIA IN DOGS

Haider Sabah Taher

Veterinary Medicine College, University of Baghdad, Iraq

Abstract

The present study was aimed to evaluate the efficiency of both bovine urinary bladder matrix (UBM) sheets and Polypropylene mesh (PPM) in the reconstruction of diaphragmatic hernias in local breed dogs. Under sedation and general anesthesia, five centimeters ring of diameter in the left muscular part of diaphragm hernias were induced and then left for one week.. The animals were divided randomly into two main equal groups (n=5). In the PPM-treatment group, the hernias were treated with implantation of PPM. While UBM-treatment group, the hernias were treated with implantation of UBM. Clinical, histopathological and gross changes were followed-up along the period of 6 weeks of study to evaluate the healing process and reconstruction of the diaphragm defects. The histopathological examination of the biopsies at end of 6th weeks post-treatment revealed that UBM treated hernias have enhanced early healing, including mononuclear cells, highly cellularity of fibroblasts proliferation, myofibroblasts and collagen deposition as well as early incorporation, degradation, and remodeling with time at area of sheets implantation. By contrast, PPM treatment group showed mononuclear infiltration, necrosis, fibro-encapsulation, remnants of mesh, and disorganized tissues were validated with the histologic score that showed the highest cellular infiltration, scaffold degradation, and neovascularization. In UBM group, only mild adhesions were found with significant deference in adhesion score between UBM and PPM, where adhered liver to diaphragm in the UBM: 1.40 ± 0.24 versus PPM: 2.80 ± 0.20, and lung to the diaphragm in the UBM: 1.80 ± 0.20 versus PPM: 2.60 ± 0.24. In conclusion; the present study confirmed that UBM scaffolds showed accelerates and improved the healing of the diaphragmatic hernia recovering and the tissue properties that might help and reducing the possibility of early failure and prevent complications associated with the implanted material.

Key words : Bovine, Urinary Bladder, Polypropylene Mesh, Chronic Diaphragmatic.

Introduction

The diaphragm is a unique skeletal muscle, it separates the abdominal and thoracic cavity, it has a vital role in both respiration and as an anatomic contribution to the lower esophageal sphincter (Lessa *et al.,* 2016). There are many lesions effect the diaphragm, which is more important the diaphragmatic hernia where the passage of the abdominal viscera into the thoracic cavity through opening or tear in diaphragm, which may be congenital or acquired (Feranti *et al.,* 2016).

Small defects can be closed using the residual diaphragm. Closure of large defects or reconstruction with extended resection of the thoracic wall, lung and pericardium normally requires the use of the prosthetic implantation. The choice of the prosthetic material for successful diaphragm reconstruction has remained a challenge in current thoracic surgical practice (Huang *et al.,* 2014).

Synthetic implants such as polypropylene and expanded polytetrafluoroethylene (ePTFE) have been used extensively in the last decades. Non-absorbable synthetic materials work with a combination of mechanical force and intense inflammatory reaction (Barua *et al.,* 2012). After implantation, using the inflammatory response leads to intense adhesions, chronic sinus (2–6%), fistula formation (0– 2%) and wound infection (2–17%). Other potential complications of synthetic meshes include mesh migration, extrusion, folding of the edges

***Author for correspondence :** E-mail : dr.hdr87@gmail.com

with visceral contact, recurrence, inflammation, seroma and chronic pain due to inflammatory response and/or nerve entrapment (Barua *et al.,* 2012).

Biosynthetic grafts seem to offer a solution to these challenging problems (Hamid *et al.,* 2016). Urinary bladder matrix (UBM) represents a biologically derived material for use in hiatal hernia repair reinforcement with the potential to improve durability of repair without incurring the risks of other reinforcement materials (Sasse *et al.,* 2016). Urinary bladder matrix (UBM) has shown effectiveness in animal studies and human clinical use for management of complex wounds and reinforcement of surgically repaired soft tissue with connective tissue remodeling in anatomic settings as diverse as esophageal, urinary bladder, pelvic floor, body wall repair, and superficial wound-healing (Afaneh *et al.,* 2015).

So that, the objectives of this study were: To evaluate effectiveness of bovine urinary bladder matrix implant on the repair and reconstruction diaphragmatic hernia in dogs compare with polypropylene mesh**,** evaluated through :Clinical evaluation,Pathological of Macro and Microscopical analysia.

3. Materials and Methods

Experimental Study Design

Ten local dogs were used in this study. The dogs were clinically healthy and weighed about 15-20 kg. They were separately housed in wire cages, given commercial pellets as food and provided with water**,** and kept in their respective cages at the College of Veterinary Medicine, University of Baghdad for 15 days for acclimatization before experimentation. The experimental animals were preventive systemic antibiotic dewormed with ivermectin (KEPRO) at a dose of 0.2mg/Kg, body weight. The experimental animals were induced the diaphragmatic defect with 5 cm in left muscular part of the diaphragm 5cm and left for seven days. After seven days, the animals of this study were divided randomly into two equal groups (n =5) as following. The first group, the hernias were treated by covering the diaphragmatic ring with onlay implantation of a sheet of xenogeneic acellular bovine urinary bladder matrix. In the second group, the hernias were treated by covering the diaphragmatic ring with onlay implantation of the Polypropylene mesh, (5 cm) in middle left side of diaphragm in the muscular part and evaluated clinically of respiratory rate, heart rate, pulse rate and macroscopically, and microscopically.

Preparation of Urinary Bladder Matrix

The whole fresh urinary bladders were harvested from the slaughtered cows at the local abattoir, and UBM-ECM prepared as a decellularized scaffold described and applied previously by Rosario *et al., (*2008) and Eberli *et al., (*2011). The urinary bladder was filled with tap water to facilitate the trimming and removing of external connective tissues and adipose tissue by scissors then washed with tap water. Tunica serosa, tunica muscularis and most of the muscularis mucosa were mechanically delaminated from the bladder tissue by scraping with blunt knife. The remaining basement membrane of the tunica mucosa and the underlying lamina propria, which collectively termed UBM, was then decellularized and disinfected by immersion the sheet in a mixture of peracetic acid (PAA) (0.1%) with ethanol (4%) for two hours. After that, the ECM was rinsed in phosphate buffered saline (PBS) (pH 7.4), then returned the pH to 7.4 containing of penicillin (100 IU/ml) streptomycin (100 ìg/ml) and amphotericin (100 ìg/ml) together at room temperature with trembling, then in deionized water two changes and finally one change in PBS. Every rinse needs 15 minus. The resulted decellularized ECM scaffolds were terminally sterilized by immersion in PAA solution (0.1%) titrated to pH 7.0 at room temperature for five hours. For ensure the decellularization, the sheet made was histological evaluated (H&E) (Totonelli *et al.,* 2012) (Fig. 1).

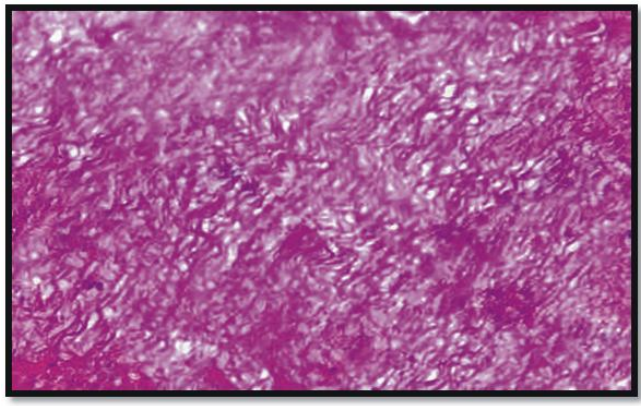

Fig. 1: Histopathological section of UBM micrograph after decellularized show wavy collagen arrowed (H&E ×40).

Polypropylene Meshes

The Polypropylene meshes, macroporous, thin wall structure, monofilament mesh, open pore (Polymesh, Betatech medical Ltd, Istanbul,Turkey) was used in the study, The mesh was cut into 6.0×6.0 cm squares.

Macroscopic Evaluation

At end of experimental after six weeks, all animals euthanized by injection overdose of ketamine. When the samples of implants were obtained at the detected period for macroscopic examination was done to inspect the presence of fibrotic adhesion of biomaterial into the

surrounding tissues, presence of infection, and any signs of implants rejection. Additionally, an assessment and classification of any adhesion formation from both the lung and abdominal contents to the diaphragm was carried out according to a frequently used scale (Butler *et al.,* 2001) and (Bellon *et al.,* 2002).

Table 1: Adhesion formation scale: macroscopic classification of adhesion to thoracic and abdominal organs (Butler *et al*., 2001; Bellon *et al*., 2002).

Score	Description
0	No adhesions
1	Minimal adhesions that could be freed by gentle blunt dissection
2	Moderate adhesions that could be freed by aggressive blunt dissection
3	Dense adhesions that required sharp dissection to free the tissue

Histopathological Evaluation

After 6 weeks of PO, all experimental animals were euthanized and sampled at reconstructed DH were harvested and the histopathological was evaluated. Underwent midline laparotomy, and the reconstructed diaphragms were excised. The excised of diaphragmatic specimens with pleura and peritoneum. The area of 1x1 cm2 was collected from three region of implant, the edge an adjacent of surrounding tissue, center of the implant and from the intermediate region between them. The samples were fixed in 10% buffered formalin solution and set in paraffin and then sectioned longitudinally and transversally to prepare 5-7 ìm thick sections and stained with hematoxylin-eosin (H&E), and Masson Trichrome stain. The analysis of the histological score of healing process progression in the site of hernias in the both treatment groups were evaluated using a scoring system as mentioned in table 3-4 illustrated by Jenkins *et al. (*2010) and Young *et al., (*2018).

Statistical Analysis

The Statistical Analysis System- SAS (2012) program was used to detect the effect of difference factors in study parameters. Least significant difference –LSD test (Analysis of Variation-ANOVA) was used to significant compare between means in this study.

Results

Gross Changes Post Treatment

The adhesion was formed in both treated groups, at 6th postoperative week between the liver and some thoracic organs such as the caudal borders of lung lobe with diaphragm. The degree of adhesion in PPM treated group was more than UBM treated group. There was significant difference in adhesion scores between the PPM and the UBM group in either liver-to-diaphragm adhesions (1.40 ± 0.24 versus 2.80±0.20 respectively) or lung-to diaphragm adhesions (1.80 ± 0.20 versus 2.60± 0.24 respectively).

Histopathological Examinations

There was presence of tendon like tissue between host diaphragm muscle and regenerated site replaced by thick collagenous tissue. However, several of newly developed muscle bindles can be noted in the mature connective tissue, some of muscle cell appeared with central nuclei myofibroblasts deposition and showed muscle bundles coat with central nuclei myofibroblasts. While in PPM treated group show the collagen fibers was became more mature with

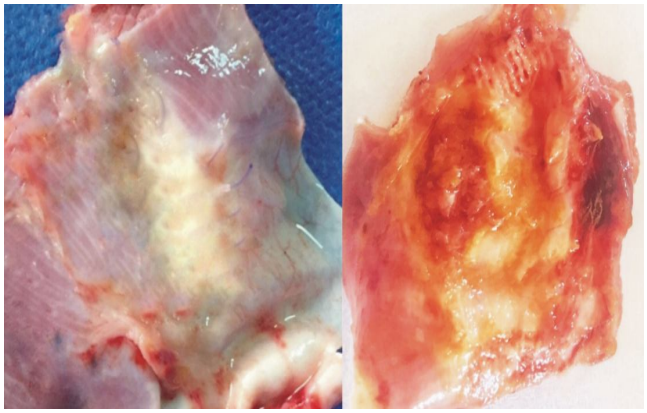

Fig. 2: (A) Photograph Show healing of the suture line and complete replacement of the patch by fibrous tissue with neovascularization in UBM treated group. **(B)** the polypropylene treated group covered with granulation tissue.

Table 3: Comparison between PPM and UBM in Adhesion formation variables study according to Adhesion score.

Adhesion formation	Mean ± SE		T-Test
	UBM	PPM	
Liver to diaphragm	1.40±0.24	2.80±0.20	0.922 *
Lung to diaphragm	1.80±0.20	2.60±0.24	0.729 *

* (P<0.05)

significant subside to mononuclear inflammatory cells infiltration. Other section showed slight fragmentation of host diaphragmatic muscle and extended of granulation tissue between muscle bundle (Thick collagen between muscle bundle invade the muscular tissue, and penetrate diaphragmatic muscular tissue and (Fig. 4.22)

The analysis of histopathological score Table (4-3) of healing progression at the site of hernias of both treatment groups were evaluated by using a scoring system adapted from Young *et al.,* (2018) gave information about Inflammation to the implant site, it give

Table 2: Histopathological scores of progression of healing process in the site of hernias (Jenkins *et al., (*2010) and Young *et al*., (2018).

Cell type/response	Score				
	0	**1**	**2**	**3**	**4**
Inflammation (PMNcells, macrophages, FBGCs)	None. No inflammatory cells presents.	Rare. (1-5 PMNs per HPF).Inflammatory cells presents<10% of surface area.	Mild infiltrate. (5-10 PM Nsper HPF).Inflammatory cells presentsin 10%-33% of surface area.	Heavy infiltrate. (>10 PMNs per HPF). Inflammatory cells presents in 33%-75% of surface area.	Packed (PMNs toonumerous to count).Inflammatory cells presents(neutrophils, macrophages, and FBGC) > 75% of surface area
Necrosis	None.	Minimal (<10% of surface area).	Mild (10%-33% of surface area).	Moderate (33%-75% of surface area	Severe (>75% of surface area
Fibrosis and fibrous encapsulation	None.No fibrous encapsulation	Minimal (<10% of surface area). Minimal encapsul ation(<10% of periphery).	Mild (10%-33% of surfacearea). Mild encapsulation (10%-33% of periphery	Moderate (33%-75% ofsurface area).Moderate encapsulation(33%-75% of periphery	Severe (>75% of surfacearea). Extensive encapsulation(>75% of periphery).
Neovascularization	Marked.Most abundant capillariespresent (>20 capillaries/HPF). Vessels penetrate intocenter of scaffold.	Moderate.Abundant capillariespresent (10-20 capillaries/HPF). Vessels penetrate intocenter of scaffold.	Mild.Many capillaries (5-10capillaries/HPF). Vessels infiltrate scaffold but none reach center of scaffold	Minimal.Few capillaries (1-5capillaries /HPF). Vesselspresent at scaffoldperiphery, no penetrationinto scaffold.	None.No capillaries or bloodvessels present
Cellular infiltration of implant	Marked (>75% of surface area).Cells penetrate into center of scaffold	Moderate (33%-75% of surface area).Cells penetrate into center of scaffold	Mild (10%-33% of surfacearea). Cells infiltrate scaffold, but none reach center.	Minimal (<10% of surface area). Cells contact periphery, no penetration into scaffold.	None.No cells in contact withscaffold.
Scaffold incorporation and degradation	Scaffold completelydegraded no histologicalevidence of originalscaffold. Tissue appears ashistologically normal	Implant material not visible, scaffold extremely degraded, difficult to distinguish scaffold from host tissue. Mild to tissue by dense, organized, fibrous connective tissue	Implant partially visible, scaffold mildly degraded. Mild degree ofincorporation into adjacent tissue, but with moderate fibrous expansion and disruption of tissue architecture	Implant visible, scaffoldpartially degraded. Minimal incorporation into adjacent tissue; complete and distinct border betweenimplant and adjacenttissue, with markedexpansion and disruption of architecture.	No incorporation, original scaffold intact, borders clearly demarcated. Implant present in entirety and distinctly separate from adjacent subcutaneoustissue (separated by clear space, edema)

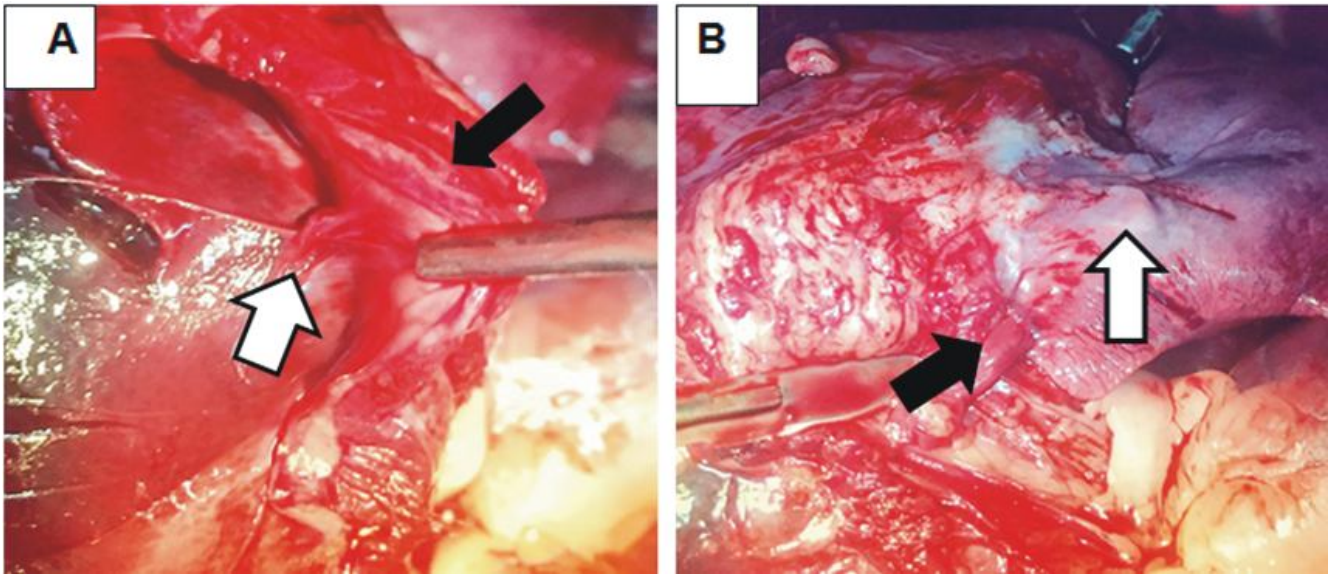

Fig. 3A: Photograph show strong adhesion between liver (white arrow) and diaphragm(black arrow) PPM treated group. **B.** Show sever adhesion between lung (white arrow) and diaphragm (black arrow) in PPM treated group.

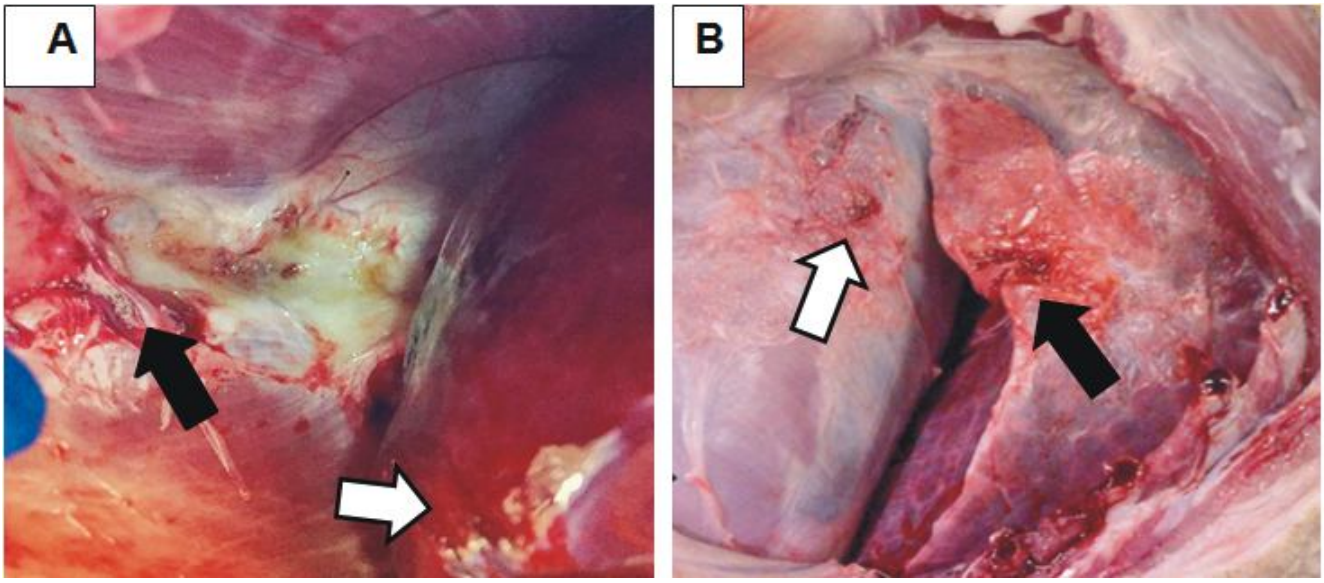

Fig. 4.A: Photograph show mild adhesion between liver and diaphragm (black arrow) UBM treated group. **B.** Show mild adhesion between lung (black arrow) and diaphragm (white arrow) in UBM treated group

information about the presence of significant difference ($P<0.05$) between both treatment groups along the studied period, it was recorded at the 6th week (1.60 ± 0.24) in UBM treatment group. In PPM-treatment group recorded (3.40 ± 0.24).

The results showed that despite the significant difference at ($P<0.05$) between both group at the 6th week. Table (4-3) reflects the of significant differences at ($P<0.05$) in both treatment groups, but the mean values of the necrosis in UBM treated group were lower (3.60 ± 0.24)and higher (3.60 ± 0.24) in PPM-treatment group.

The analysis of histological scores illustrated that the mean values of Fibrosis and fibrous encapsulation were lower in UBM treated group, while, became higher in PPM-treated group, with a significant differences ($P<0.05$) in both groups along the period of the study. In UBM treatment group(1.40 ± 0.24) lower than PPM group (3.00 ± 0.31).

In which the mean value of cellular invaded to the whole of scaffold was higher in UBM than PPM treated group and began from peripheral to the center, it was recorded (1.00 ± 0.28) in PPM-treatment group. In UBM-treatment group(1.40 ± 0.24), mean value of cells infiltrated of the scaffold higher than PPM treated group.

In the present study, the degradation of PPM-implants was slower than of UBM-implants. Six weeks post-

Table 4: Comparison between PPM and UBM in Reaction variables study according to histological score.

Reaction	Mean ± SE		T-Test
	PPM	UBM	
Inflammation (PMN cell, lymphocytes, plasma cells, macrophages, FBGCs)	3.40±0.24	1.60±0.24	0.798 *
Necrosis	3.60±0.24	1.40±0.24	0.798 *
Fibrosis and fibrous encapsulation	3.00±0.31	1.40±0.24	0.922 *
Scaffold incorporation degradation	3.20±0.20	1.60±0.24	0.729 *
Cellular infiltration of Implant	3.40±0.24	1.40±0.24	0.798 *
Neovascularization	3.40±0.24	1.40±0.24	0.798 *

* ($P<0.05$).

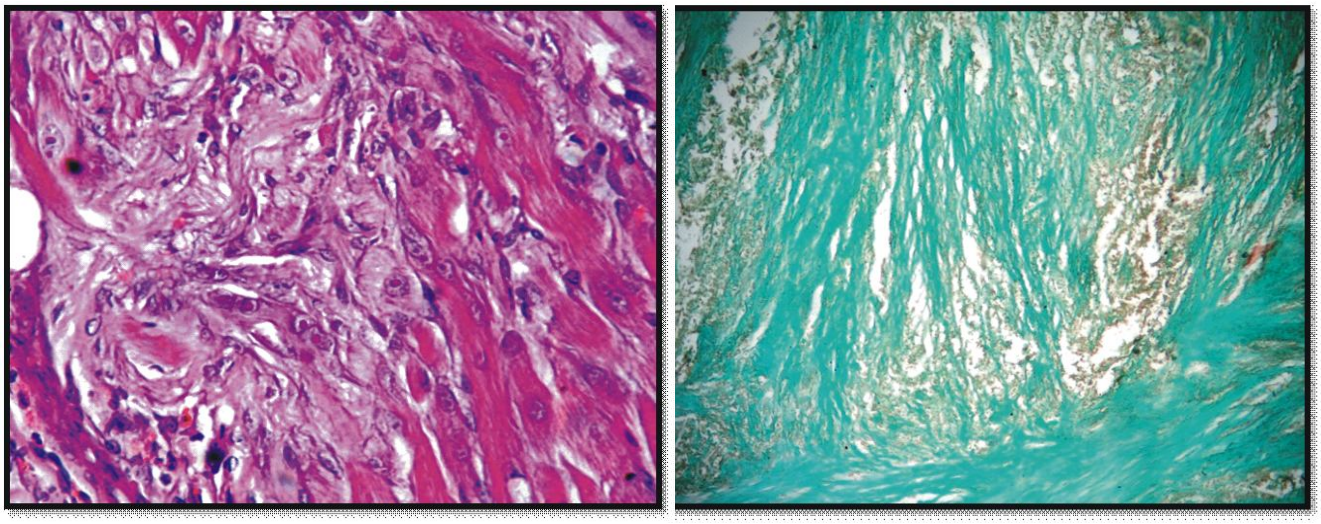

Fig. 5: Histopathological section of UBM-treated diaphragmatic hernia, 6 weeks post implantation, **A**, show muscle bundles coat with central nuclei myofibroblast arrowed. (H&E stain X40). **B**, show mature and regular granulation tissue and thick collagen arrowed. (Masson trichrome stain.

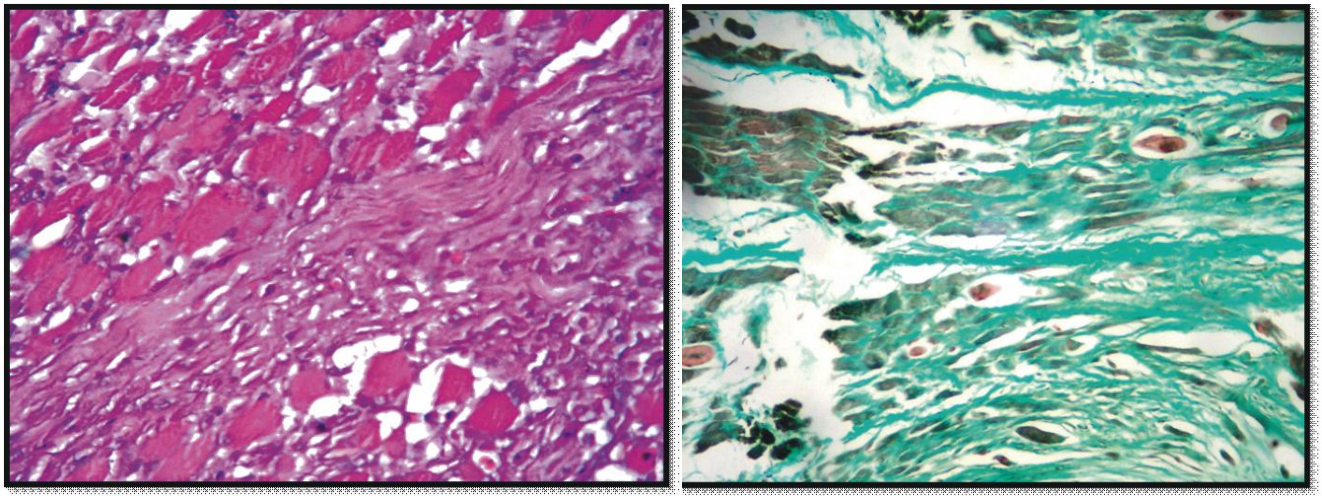

Fig. 6: Histopathological section of PPM-treated diaphragmatic hernia 6 weeks post implantation , A, show , thick collagen layer (long arrow) separated the host diaphragm muscle (short arrows). (H&E stain X20). B, **,** show , vascular granulation tissue arrowed with wavy collagen fibre Masson trichrome stain×40.

implantation, PPM-implants visible, scaffold partially degraded. The results confirmed the presence of significant differences ($P<0.05$) between both group for period of study. The mean values in UBM is low (1.60 ± 0.24) and superiority in PPM-implants group were (3.20 ± 0.20).

The analysis score of neovascularization that reflect the progress of blood vessels penetration of the scaffold, which reported significant differences ($P<0.05$) between both groups at 6th week which shows higher means in

PPM treatment group (3.40 ± 0.24) than that in UBM-treatment group (1.40 ± 0.24).

Discussion

When using of both UBM implant and PPM implants for treatment of Hiatus hernias causes the activation of inflammatory process, giant cells aggregation, in addition to its role in the acceleration of formation of new blood vessels. Amigo *et al.,* (2019). As well as, the using of UBM for muscles repair improved the muscle regeneration with myofibroblasts following muscle tissue damage through augmented myogenic progenitor cells proliferation Song *et al.,* (2013). UBM-implants enhanced the cellular integrity and induces early inflammatory cells infiltration in early phase of implantation for hernia repair in rabbits compared to the untreated tissues Eberli *et al.,* (2011).

who observed that the PPM implants occur resistant to biological degradation Novitsky *et al.,* (2007) , while, UBM scaffolds could not be histologically identified at 3 months; it was proved by the authors in previous publications at 2 months (Riganti *et al*., 2016). The UBM-implants rapidly degraded, more rapid turnover and remodeling Remlinger *et al.,* (2013).

The degradation process has a significant biological activity which stimulates the releasing of the inherent bioactive constituents (Badylak *et al.,* 2009) subsequently promote tissue neovascularization and host-cell deposition (Gilbert *et al.,* 2007) through encouraging cells attachment, proliferation, differentiation, maturation and angiogenesis (Wang *et al.,* 2009). The biological scaffold encapsulation indicates an accelerated progression of the inflammatory response. At this time, the proteoglycans had predominate at early stage of granulation tissue but later collagen type-III, as a fibroblasts production, predominates and forms the fibrous capsule around biological implant. Additionally Anderson *et al.,* (2004 and 2008). The dense fibrous capsule which is formed around implant during remodeling was responsible for the firm incorporation between the implant and the host tissue. These results give the reason for UBM implant in corporation prior to PPM implant Murat Samli *et al. (*2004) and Abouelnaser, (2008).

The UBM implants have been used for hiatal hernia repair in human, confirmed the ability of this type of bioscaffolds to facilitate a constructive remodeling process that lead to reduce scarring and facilitates the restoration of normal site appropriate tissue Sasse *et al.* (2016). In addition, the formation of dense collagen fibers with MNCs infiltrations around blood vessels at treated site compared to control group at 8th week post-implantation of UBM for tenorrhaphy AL-Abedi, (2014).

UBM patch was observed throughout the remodeling process at week 4th and 8th after implantation Remlinger *et al.,* (2013).

References

Abouelnasr, K.S., A.E. Zaghloul and G.I. Karrouf (2014). Comparative evaluation of glycerolized bovine pericardium implant with prolene mesh for closure of large abdominal wall defects in dogs. *Iranian J. of Veterinary Research*, **15(3):** 211-217.

Afaneh, C., D. Gerszberg, E. Slattery, D.S. Seres, J.A. Chabot and M.D. Kluger (2015). Pancreatic cancer surgery and nutrition management: a review of the current literature. *Hepatobiliary surgery and nutrition*, **4(1):** 59

AL-Abedi, A.H. (2014). Effect of bovine urinary bladder sub-mucosa on tendon reconstruction in equine species. Msc. Thesis in Veterinary Surgery. University of Baghdad. Baghdad–Iraq.

Amigo, N., C. Zubieta, J.M. Riganti, M. Ramirez, P. Renda, R. Lovera and T.W. Gilbert (2020). Biomechanical Features of Reinforced Esophageal Hiatus Repair in a Porcine Model. *journal of surgical research*, **246:** 62-72.

Anderson, J.M., G. Cook, B. Costerton, S.R. Hanson, A.H. Pettersen, N. Jacobsen, R.J. Johnson, R.N. Mitchell, M. Pasmore, F.J. Schoen, M. Shirtliff and P. Stoodley (2004). Host reactions to biomaterials and their 84 evaluation. Chapter four. Biomaterials Science, 2nd Edition Copyright © 2004 Elsevier Inc. All rights reserved: 293-204.

Badylak, S.F. and T.W. Gilbert (2008, April). Immune response to biologic scaffold materials. In *Seminars in immunology* **20(2):** 109-116. Academic Press.

Bellón, J.M., F. Jurado, F. García Moreno, C. Corrales, A. Carrera San Martín and J. Buján (2002). Healing process induced by three composite prostheses in the repair of abdominal wall defects. *Journal of Biomedical Materials Research: An Official Journal of The Society for Biomaterials, The Japanese Society for Biomaterials, and The Australian Society for Biomaterials and the Korean Society for Biomaterials*, **63(2):** 182-190.

Butler, C.E., F.A. Navarro and D.P. Orgill (2001). Reduction of abdominal adhesions using composite collagen GAG implants for ventral hernia repair. *Journal of Biomedical Materials Research: An Official Journal of The Society for Biomaterials, The Japanese Society for Biomaterials, and The Australian Society for Biomaterials and the Korean Society for Biomaterials*, **58(1):** 75-80.

Eberli, D., A. Atala and J.J. Yoo (2011). One and four layer acellular bladder matrix for fascial tissue reconstruction. *Journal of Materials Science: Materials in Medicine*, **22(3):** 741-751

Gilbert, T.W., S. Gilbert, M. Madden, S.D. Reynolds and S.F. Badylak (2008). Morphologic assessment of extracellular matrix scaffolds for patch tracheoplasty in a canine model.

The Annals of thoracic surgery, **86(3):** 967-974.

Huang, P., G. Cheng, H. Lu, M. Aronica, R.M. Ransohoff and L. Zhou (2011). Impaired respiratory function in mdx and mdx/utrn+/" mice. *Muscle & nerve*, **43(2):** 263-267.

Jenkins, E.D., V. Yom, L. Melman, L.M. Brunt, J.C. Eagon, M.M. Frisella and B.D. Matthews (2010). Prospective evaluation of adhesion characteristics to intraperitoneal mesh and adhesiolysis-related complications during laparoscopic re-exploration after prior ventral hernia repair. *Surgical endoscopy*, **24(12):** 3002-3007.

Lessa, T.B., D.K. de Abreu, B.M. Bertassoli and C.E. Ambrósio (2016). Diaphragm: a vital respiratory muscle in mammals. *Annals of Anatomy-Anatomischer Anzeiger*, **205:** 122-127.

Mehta, A., R. Afshar, D.L. Warner, A. Gardner, E. Ackerman, J. Brandt and K.C. Sasse (2017). Laparoscopic rectopexy with urinary bladder xenograft reinforcement. *JSLS: Journal of the Society of Laparoendoscopic Surgeons*, **21(1)**.

Murat Samli, M., M. Demirbas, C. Guler, F. Aktepe and C. Dincel (2004). Early tissue reactions in the rat bladder wall after contact with three different synthetic mesh materials. *Br. J. of Urol.*, **93(4):** 617–621.

Novitsky, Y.W., A.G. Harrell, J.A. Cristiano, B.L. Paton, H.J. Norton, R.D. Peindl and B.T. Heniford (2007). Comparative evaluation of adhesion formation, strength of ingrowth, and textile properties of prosthetic meshes after long-term intra-abdominal implantation in a rabbit. *Journal of Surgical Research*, **140(1):** 6-11.

Remlinger, W. (2013). *Analyse von Sichteinschränkungen im Fahrzeug* (Doctoral dissertation, Technische Universität München).

Riganti, J.M., F. Ciotola, A. Amenabar, D. Craiem, S. Graf, A. Badaloni and A. Nieponice (2016). Urinary bladder matrix scaffolds strengthen esophageal hiatus repair. *Journal of Surgical Research*, **204(2):** 344-350.

Rosario, D.J., G.C. Reilly, E. Ali Salah, M. Glover, A.J. Bullock and S. Macneil (2008). Decellularization and sterilization of porcine urinary bladder matrix for tissue engineering in the lower urinary tract. *Regen. Med*., **3:**145.

Sasse, K.C., D.L. Warner, E. Ackerman and J. Brandt (2016). Hiatal hernia repair with novel biological graft reinforcement. *JSLS: Journal of the Society of Laparoendoscopic Surgeons*, **20(2)**.

Song, Z., Z. Peng, Z. Liu and J. Yang (2013). Reconstruction of abdominal wall musculofascial defects with small intestinal submucosa scaffolds seeded with tenocytes in rats. Tissue Eng., Part A, **19(13-14):**1543–1553.

Totonelli, G., P. Maghsoudlou, M. Garriboli, J. Riegler, G. Orlando, A.J. Burns and M. Turmaine (2012). A rat decellularized small bowel scaffold that preserves villus-crypt architecture for intestinal regeneration. *Biomaterials*, **33(12):** 3401-3410.

Young, D.A., N. Jackson, C.A. Ronaghan, C.E. Brathwaite and T.W. Gilbert (2018). Retrorectus repair of incisional ventral hernia with urinary bladder matrix reinforcement in a long-term porcine model. *Regenerative medicine*, **13(4):** 395-408.

Wang, C.Q., T. Tran, B. Montera, R. Karlnoski, J. Feldman, M.H. Albrink and V. Velanovich (2019). Symptomatic, Radiological, and Quality of Life Outcome of Paraesophageal Hernia Repair With Urinary Bladder Extracellular Surgical Matrix: Comparison With Primary Repair. *Surgical laparoscopy, endoscopy & percutaneous techniques*, **29(3):** 182-186.